5th International Conference on Durability of Concrete Structures
Jun 30–Jul 1, 2016
Shenzhen University, Shenzhen, Guangdong Province, P.R.China

Electrical Response of Mortar Saturated with NaCl Solutions under Freeze–Thaw Cycles

Yi Wang, Fuyuan Gong, and Tamon Ueda
Department of Civil Engineering, Hokkaido University

Dawei Zhang
College of Civil Engineering and Architecture, Zhejiang University

ABSTRACT

This paper presents the test results of electrical response of mortar saturated with sodium chloride (NaCl) solutions under freeze–thaw cycles (FTCs). To quantitatively evaluate the salt frost damage of mortar based on its electrical response, mesoscale samples are prepared to assure the uniform pore solution concentration. The reduction of electrical resistivity shows the same tendency with elastic modulus, but with less degree. The investigation shows that electrical resistivity of mortar decreases with temperature and the phase changes can be observed based on their relationship. The freezing and thawing points decreasing with increment of solution concentration can be found, but their variations with FTCs are not significant. Basically, along with frost damage development, the electrical resistivity of mortar at 23 and –28°C is decreasing with FTCs. However, for lower water-to-cement ratio and higher NaCl concentration solution exposed samples, contrary tendency are observed. In addition, with FTCs, there is no clear change for the activation energy of DI water case, whereas the decreasing tendency is observed in the cases of 5 and 15% NaCl solution. Therefore, the electrical properties are important for understanding the salt frost damage, but a comprehensive parameter to quantify the damage is still in need.

1. INTRODUCTION

In cold and wet regions, transportation-related concrete structures, such as bridges, roadways, and walkways, are fragile to freeze–thaw cycles (FTCs) (Litvan, 1976). In order to protect the safety of vehicles and pedestrians, ice on the surface concrete will be removed by spraying deicing agents [e.g., sodium chloride (NaCl)]. But, the deicing agents can accelerate the frost damage of concrete, which arising much concern in recent years (Valenza & Scherer, 2007). In addition to salt scaling which spoils the appearance of the concrete, more importantly, internal frost damage is threat to the safety. The salt frost damage can increase the permeability of concrete, which promotes the penetration of aggressive species, resulting in the corrosion of reinforcement. Thus, there is in need to investigate the frost resistance of concrete combined with salt ingress. However, there is still no agreement about the damage mechanism until now (Liu & Hansen, 2015; Wu, Shi, Gao, Wang, & Cao, 2014).

According to acoustic emission results, Farnam, Bentz, Sakulich, Flynn, and Weiss (2014) found that the most severe frost damage is not happened at around 3% of NaCl solution but at 15%, which reveals that the damage process is much more complicated than the existing models explained (Sun & Scherer, 2010). However, from the deformation measurement (Zeng, Fen-Chong, & Li, 2014), no severe damage was observed in the case of 15% NaCl saturated sample in sealed condition. Besides, our previous closed freeze/thaw test results show that the strength and stiffness of NaCl solution saturated mortar degrade with FTCs (Wang, Gong, Ueda, & Zhang, 2016a). Therefore, to understand the damage mechanism, an alternative measurement to evaluate the damage of concrete is needed.

Recently, investigating the frost damage of concrete by electrical measurement was proposed as a great potential methodology (Sato & Beaudoin, 2011). This technique was applied to study concrete for decades (Whittington, McCarter, & Forde, 1981); moreover, it is believed that the electrical resistivity of concrete is related to the pore characteristics, pore solution composition, saturation degree, and temperature (Weiss, Snyder, Bullard, & Bentz, 2012). Since ice formation is essential for understanding the frost damage of concrete (Gong, Wang, Zhang, & Ueda, 2015), electrical measurements was applied to estimate the ice content below freezing point (Cai & Liu, 1998; Wang, Gong, Zhang, & Ueda, 2016b). In addition, Wang, Zeng, Wang, Yao, and Li (2014) attempted to use the maximum electrical resistivity to evaluate the frost damage of cement paste immersed to water with FTCs. On the other hand, Farnam, Todak, Spragg, and Weiss (2015) studied the mortar saturated with

different concentration NaCl solution and the electrical resistivity change at reference temperature (20°C) was considered to be the damage index, but only the first FTC was considered. As they use the macroscale samples for testing, the salt frost damage may be not uniform along the depth of sample. So, evaluation of salt frost damage of mortar with FTCs needs further investigation.

This study investigated the electrical response of mortar in mesoscale saturated with deionized (DI) water, 5 and 15% NaCl solutions under FTCs. The main purpose of this paper is to determine whether the electrical measurements can be applied to evaluate the salt frost damage under FTCs. The results from three-point bending test of normalized elastic modulus were compared with the electrical response under FTCs.

2. TEST PROGRAMS

2.1 Specimen preparation

Mortar specimens were used in this experimental program. Mix proportions were based on ACI Committee (1991) design, as shown in Table 1, with different water-to-cement ratio (*w*/*c*), excluding coarse aggregate. The materials include Ordinary Portland cement, the physical properties and chemical compositions are presented in Table 2. The size of fine aggregate is 1.2 mm or lesser and its density is 2.67 g/cm^3. To promote frost damage, no air-entraining agent was incorporated. After proper mixing, it was cast into 40 mm × 40 mm × 160 mm form and cured for 24 h prior to removing the form. Once demolded, specimens were cured under water for 90 days at the temperature of 20–23°C. Then, the specimens were cut into size of 70 mm × 30 mm × 5 mm after curing. The mesoscale size was chosen because the pore solution concentration can be assumed to be uniform, because salt frost damage could be quantitatively understood.

Table 1. Mix proportions and porosity of mortar.

Water/cement Ratio	Water kg/m^3	Cement kg/m^3	Fine aggregate kg/m^3
0.7	207	296	1090
0.5	207	414	990
0.3	207	690	755

The test preparation involves two parts. One is for electrical test, whereas the other is for three-point bending test. The preparation procedures of electrical test samples were shown in Figure 1. First, the electrodes were attached to mortar samples with conductive paste [see Figure 1(a)]. Once the conductive paste is cured, to solidify the interface bonding of electrodes and specimens, the epoxy resin was also deployed to cover the conductive paste and electrode [see Figure 1(b)]. After 1 week curing of epoxy resin, the samples were placed into a vacuum desiccator for another week to obtain dried condition. After drying, they were sealed with a plastic bag [see Figure 1(b)] to prevent moisture transfer and kept in a vacuumed chamber until testing. In order to obtain fully saturated specimens, the solutions were vacuuming 20 min to remove the air first; then, the samples were immersed into DI water, 5 and 15% NaCl solutions, respectively [see Figure 1(c)] and continuous vacuuming for 1 h. After that, the samples remained in solution for 7 days at room temperature until they were taken out. To prevent moisture transfer, they were sealed with saran and tape after surface dried by towel paper [see Figure 1(d)]. The preparation of three-point bending test sample is similar to the above description except the part of electrode and epoxy resin, the details can be seen in our previous report (Wang et al., 2016a).

2.2 Electrical and freeze–thaw cycles tests

In the electrical test, the electrical resistance of specimen was measured by alternating current (AC) two-point method with FTCs (Wang et al., 2016b). The frequency of the alternating current is 1 kHz, and the test data were collected every 10 s by computer continuously. Before the test, the electrical resistance of conductive paste under FTCs was measured and the value was around 0.5 Ω, which can be neglected compared with electrical resistivity of mortar samples. To consider the geometrical effect, the electrical resistivity of the specimen is

$$\rho = \frac{AR}{L} \tag{1}$$

where R is the resistance of the specimen, A is the cross-sectional area, and L is the length of the specimen.

Table 2. Physical properties and chemical compositions of cement (OPC).

	Specific gravity		Specific surface (cm^2/g)		Compressive strength (MPa)			
					3 days		7 days	28 days
Physical properties	3.16		3350		31.3 ± 1.63		47.1 ± 1.76	63.5 ± 1.88
Composition	CaO	SiO_2	Al_2O_3	Fe_2O_3	SO_3	MgO	K_2O	Na_2O
Content (%wt)	64.20	21.40	5.51	2.92	2.03	1.74	0.36	0.21

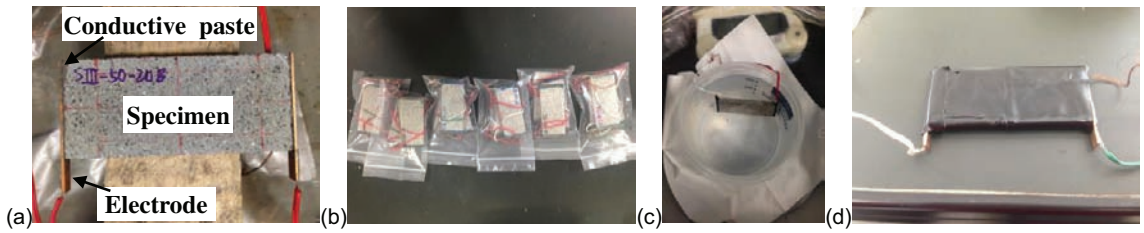

Figure 1. Prepared specimen details 70 mm × 30 mm × 5 mm.

The prepared specimens were placed into an environmental chamber to undergo FTCs, and the freeze–thaw temperature history of the chamber can be seen in Figure 2. Since the specimens were sealed, the relative humidity inside the chamber has no effect on the frost damage process; therefore, only the temperature was controlled and measured by a temperature sensor recorded by computer. The temperature started at 23°C for 100 min, then decreased by 0.25°C per minute until it reached the minimum temperature –28°C and remained constant for 100 min, and then increased by 0.25°C per minute until the maximum temperature 23°C. After certain repeated FTCs, the specimens were taken out from the environment chamber and kept at room temperature before three-point bending test.

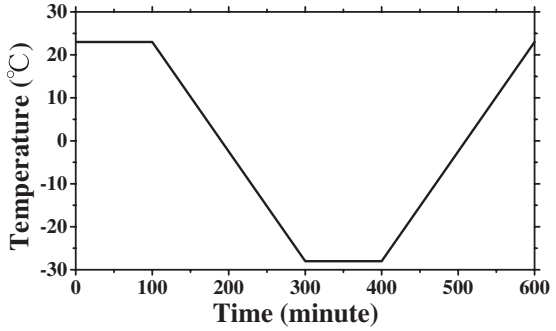

Figure 2. Temperature history (one cycle).

2.3 Three-point bending test

After exposed to FTCs, the specimens were unsealed. Then, they were placed at vacuumed chamber for 3 months. To control the crack propagation, notch with 5 mm depth were made in the two sides of specimen central cross-section (it becomes 70 mm × 20 mm × 5 mm finally [Figure 3(b)]. As can be seen in Figure 3(a), the bending span was set 50 mm and deflection was measured by LVDTs located at the centre of the specimens and supporting points. In addition, the loading rate was set as 0.001 mm/s. The elastic modulus was calculated based on JCI Standard (2003), as following equations;

$$E = \frac{P_{1/3} l^3}{4\delta_{1/3} b h^3} \quad (2)$$

where E is the elastic modulus in megapascal, P is the maximum load in Newton, l is the bending span in millimeters, b is the width, and h is the thickness of the specimen in millimeters. $P_{1/3}$ is the one-third of the maximum load, $\delta_{1/3}$ is deflection of specimen at one-third of maximum load.

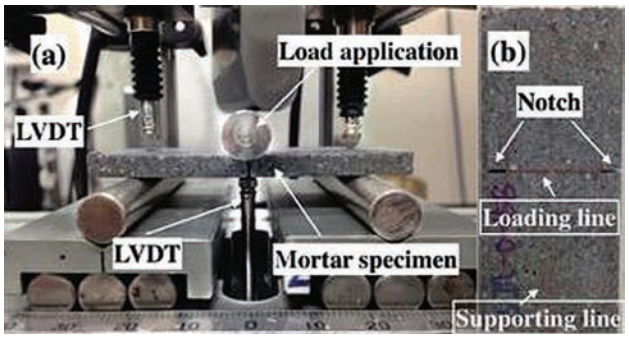

Figure 3. Three-point bending test set up.

3. RESULTS AND DISCUSSIONS

3.1 Electrical resistivity of specimen under FTCs

During FTCs, the electrical resistivity of specimens was changing with temperature. As shown in Figure 4, the measured electrical resistivity was presented as a function of time. Since the temperature was also changing with time, the relationship between electrical resistivity and temperature was further plotted with regard to FTCs (see Figure 5). The freezing and thawing points can be seen from the slope change of the curves. Because once ice nucleates in meso- and macropores, the amount of movable ions would be reduced, as a result, the electrical resistivity of mortar increases dramatically. Clearly, there is a big difference among each concentration of NaCl solution saturated specimens. As shown in Figure 5, at reference temperature (23°C), the electrical resistivity reduces with increasing of NaCl concentration. However, the 5% NaCl case specimen reached the maximum electrical resistivity at the lowest temperature except for $w/c = 0.7$ cases. The pore characteristics of hydrated products may be accounted as the reason. At the lowest temperature, water in pores partially forms to ice, and the salt crystallization is also possible to occur to fill the pores. As a result, the amount of movable

ions in 5% NaCl saturated samples with *w*/*c* = 0.3 and 0.5 would less than in DI water saturated samples as some pores are blocked by the ice and salt. However, for *w*/*c* = 0.7 case, 5% NaCl saturated samples still has good connectivity under freezing because of more porous nature and can be more conductive than in DI water because larger amount of ice would form for sample with DI water. In addition, for each *w*/*c* samples, the electrical resistivity decreases with *w*/*c* at reference temperature because of the greater amount of water in the samples. It is worthy to note that there were no additional phase changes (e.g., formation of Friedel's salt and crystallization of NaCl crystal) been observed during the freezing and thawing even for 15% NaCl saturated samples, which is different from Farnam et al. (2015)'s results. This implies that the additional phase change depends on the chemical composition of cement pastes (Baroghel-Bouny, Wang, Thiery, Saillio, & Barberon, 2012), which needs further investigation. Besides, after the ice nucleation, the non-linear curve of electrical resistivity–temperature relationship indicates that the amount of ice formed increases non-linearly. From previous results (Wang et al., 2016a; Wu et al., 2014), we understand that the samples contain 5% NaCl solution have more severe damage than DI water case, but in theory, the ice amount in 5% NaCl solution saturated sample is less than in DI water saturated sample. Since the range

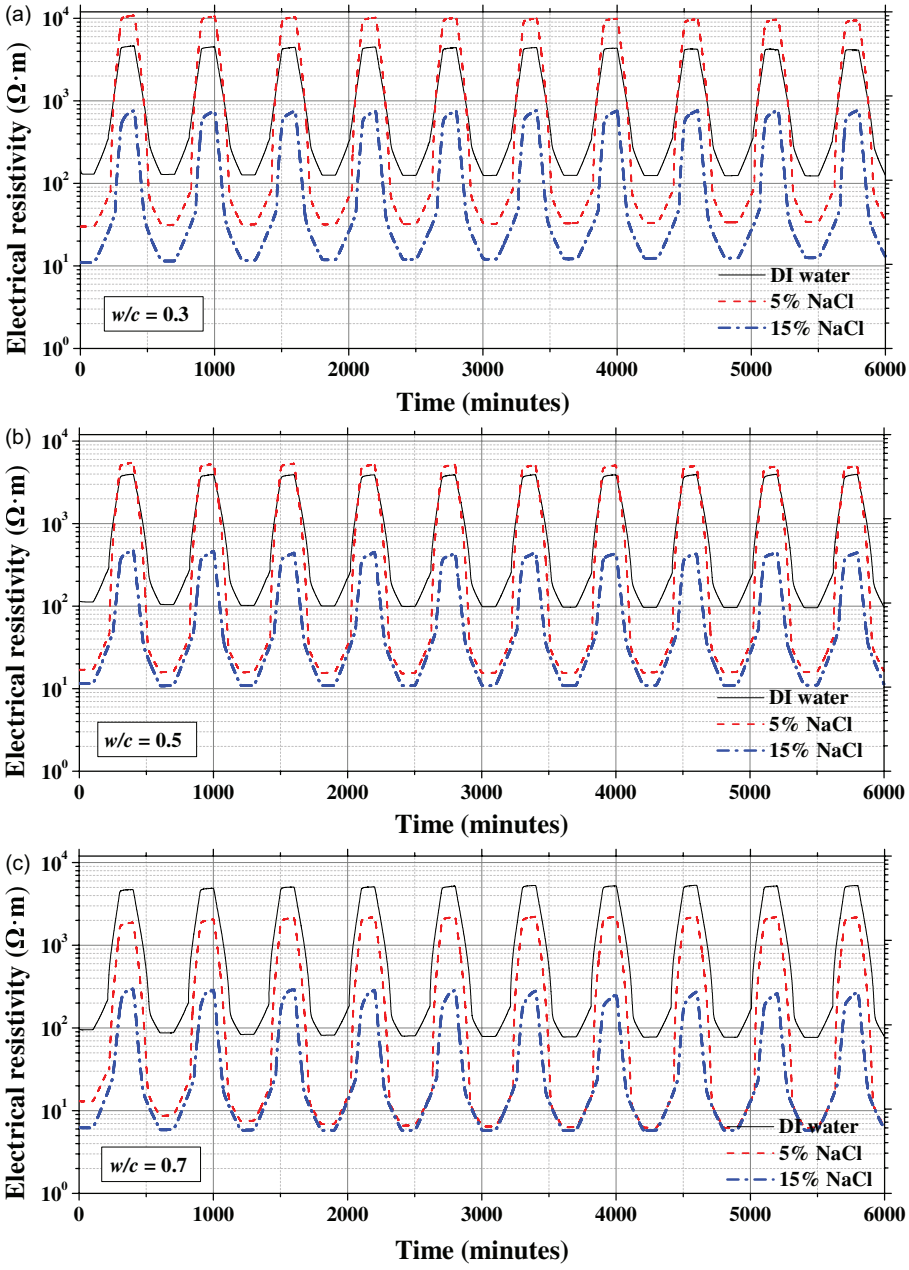

Figure 4. Electrical resistivity changes under freeze–thaw cycles (a) *w*/*c* = 0.3, (b) *w*/*c* = 0.5, and (c) w/c = 0.7

of electrical resistivity in the case of 5% is highest in Figure 4, it was believed that salt crystallization contributed to the electrical resistivity increase as well. However, no obvious change due to salt crystallization was observed. Therefore, it was assumed that the salt crystallization is also possible to occur at subzero temperature if it initiates gradually.

3.2 Electrical resistivity at reference temperature

According to the study of Farnam et al. (2015), electrical resistivity at reference temperature can be used to evaluate the frost damage, whereas Wang et al. (2014) regarded the maximum electrical resistivity as the parameter of damage. Therefore, in this paper, as shown in Figures 6 and 7, normalized electrical resistivity at temperatures 23 and –28°C were considered, respectively. The normalized electrical resistivity means the ratio of electrical resistivity with FTCs to electrical resistivity at the first cycle. Electrical resistivity at reference temperature (23°C) and lowest temperature (-28°C) at first cycle are presented in Table 3. Figures 6 and 7 show that along with frost damage development, the electrical resistivity of mortar at 23 and –28°C decreases. However, for 5 and 15% NaCl concentration solution exposed samples with w/c = 0.3, contrary tendency were observed at 23°C. The increase tendency was also observed at -28°C in the case of DI water and 5% NaCl solution exposed samples with w/c = 0.7. It indicates that the frost damage in the cases of 5 and 15% NaCl solution saturated samples with w/c = 0.3 were not significant, because of the lesser amount of moisture and salt. Besides, for the samples saturated with NaCl solutions, the chloride binding reduced the movable ions content and increased the electrical resistivity. For the samples with w/c = 0.5 and 0.7, even the chloride binding also occurs, the salt frost damage was more severe, so the electrical resistivity showed decrease tendency.

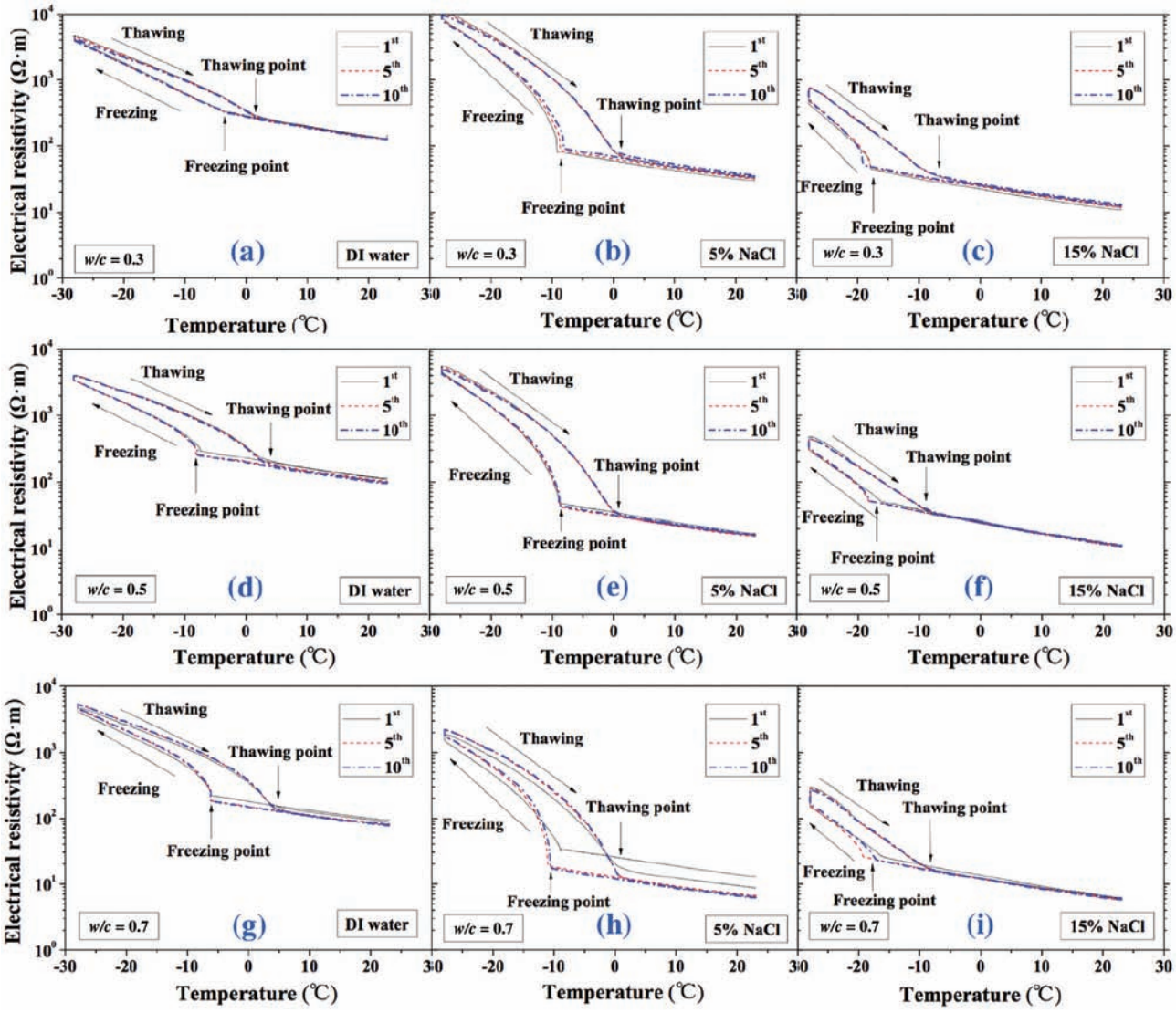

Figure 5. Electrical resistivity changes with temperature.

Table 3. Electrical resistivity at reference temperature (23°C) and lowest temperature (–28°C) at first cycle.

	Electrical resistivity at temperature 23°C (Ωm)			Electrical resistivity at temperature (-28(C (Ωm)		
	w/c = 0.3	*w/c* = 0.5	*w/c* = 0.7	*w/c* = 0.3	*w/c* = 0.5	*w/c* = 0.7
DI water	129.59	112.14	95.17	4622.47	3986.5	4745.47
5% NaCl	30.249	17.15	13.01	10,835.95	5500.58	1879.03
15% NaCl	11.03	11.57	6.23	762.15	476.87	296.41

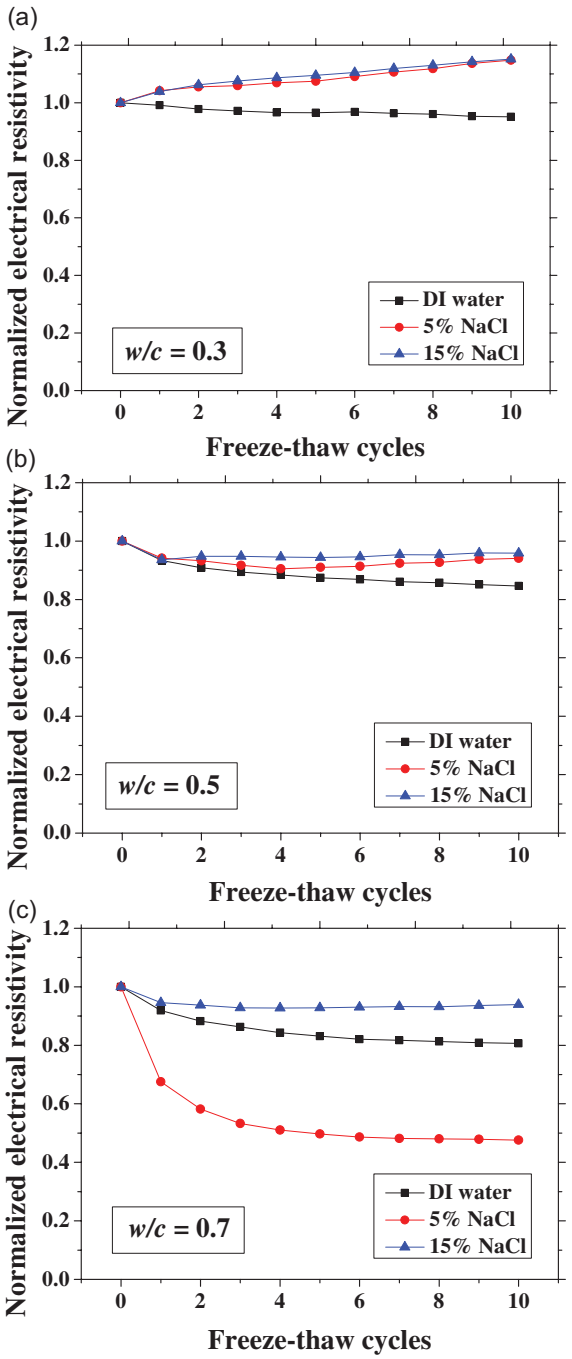

Figure 6. Electrical resistivity at reference temperature (23°C) changes with FTCs. (a) *w/c* = 0.3, (b) *w/c* = 0.5, and (c) w/c = 0.7.

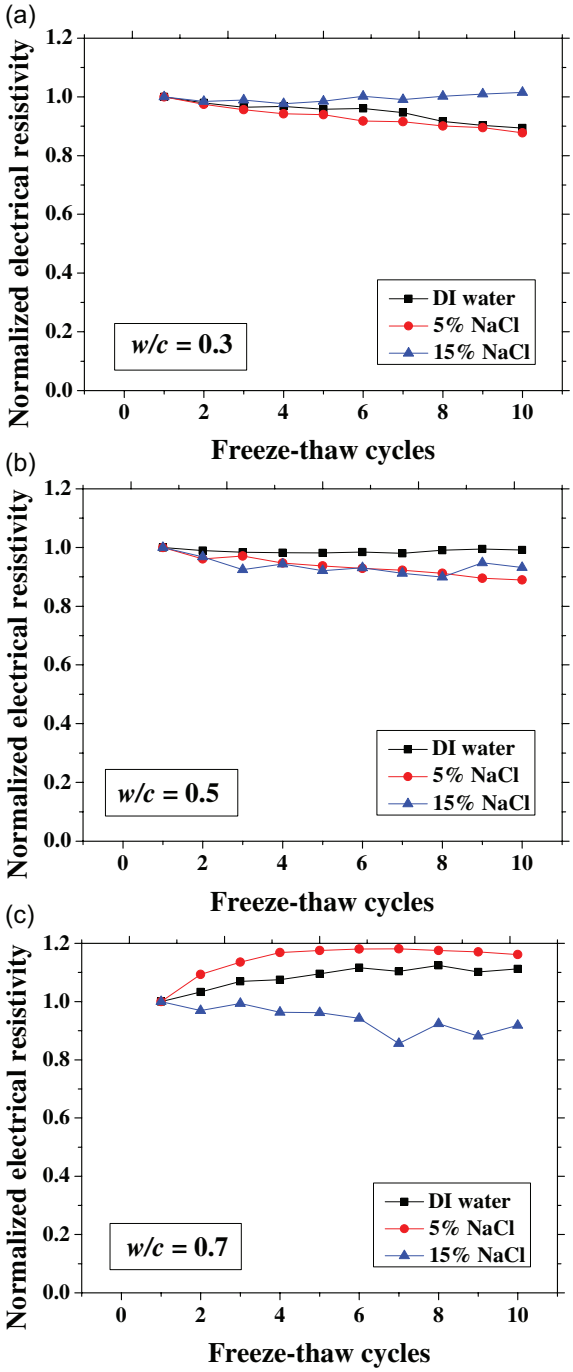

Figure 7. Electrical resistivity at lowest temperature (–28°C) changes with FTCs. (a) *w/c* = 0.3, (b) *w/c* = 0.5, and (c) *w/c* = 0.7.

However, for the case of DI water and 5% NaCl solution exposed samples with $w/c = 0.7$, the increase of electrical resistivity at the lowest temperature was due to more severe frost damage. Although the frost damage can increase the connectivity and decrease the electrical resistivity, the sample with $w/c = 0.7$ had good connectivity before frost damage, so this effect has less influence on the electrical resistivity. Instead, because of the severe damage, the increasing of porosity yields the reduction of saturation degree, which increases the electrical resistivity.

3.3 Activation energy changes with FTCs

Activation energy of mortar sample is a parameter to quantify the sensitivity of electrical resistivity to temperature and it is mainly correlated to the pore characteristics (Liu & Presuel-Moreno, 2014). The value of activation energy for fully saturated samples ($E_{a,s}$) can be calculated as Eq. (3) (Chrisp, Starrs, McCarter, Rouchotas, & Blewett, 2001; Wang et al., 2016b)

$$E_{a,s} = \frac{-R_g \ln\left(\frac{\sigma_{T,s}}{\sigma_{ref,s}}\right)}{\frac{1}{T} - \frac{1}{T_{ref}}} \quad (3)$$

where $\sigma_{T,s}$ is the electrical conductivity of fully saturated mortar sample at the absolute temperature T, $\sigma_{ref,s}$ is the electrical conductivity of fully saturated mortar sample at the absolute reference temperature T_{ref} and R_g is the universal gas constant (8.314 J/mol/K).The obtained activation energy results were shown in Figure 8.

The higher w/c, the higher volume ratio of moisture which samples can contain. For DI water cases, activation energy decreases with w/c. In the cases of w/c = 0.7, the activation energy increases with NaCl solution concentration. The reason is due to the formation of Friedel's salt consumed water and movable ions. In particular, for higher concentration exposed samples, the absorbed moisture content is lesser because the formation of Friedel's salt can fill the pores and the amount of salt increases with NaCl concentration (Wang, Gong, Zhang, & Ueda, 2016c). Although the concentration of remaining pore solution is high, the sensitivity to temperature would increase. Besides, because of less amount of Friedel's salt crystallization in the cases of w/c = 0.3 and 0.5, the activation energy of the two saturated with 5% NaCl are similar, but for 15% NaCl case, the differences become obvious due to the salt crystallization and total moisture amount. With frost damage development, both connectivity of porosity and connectivity of pores would increases, because activation energy decreases with FTCs. When the porosity and connectivity increased, the electrical

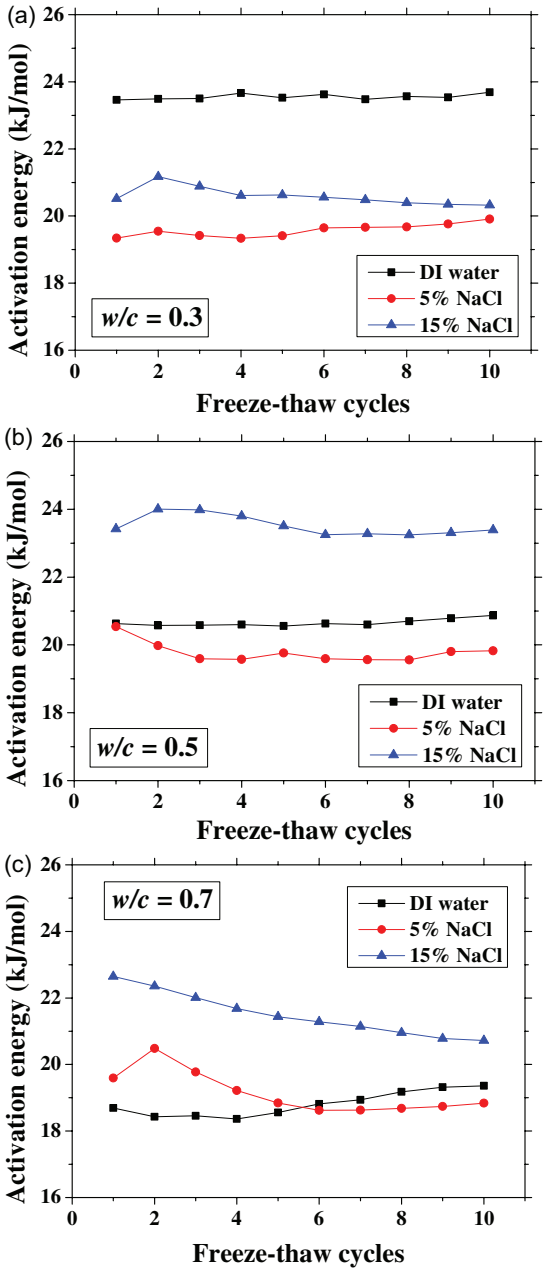

Figure 8. Activation energy of specimens changes with FTCs. (a) $w/c = 0.3$, (b) $w/c = 0.5$, and (c) $w/c = 0.7$.

resistivity at reference temperature decreases. According to the study of Liu and Presuel-Moreno (2014), for DI water saturated concrete samples, there is a relationship between the activation energy and electrical resistivity at reference temperature. Once the electrical resistivity at reference temperature decreased due to the frost damage, the activation energy would decrease correspondingly. However, after frost damage, the degree of saturation would decrease since the deformation and cracks caused the connection of air voids and increase volume of air voids. Besides, it is known that the activation energy

of mortar would increase with the reduction of water saturation degree (Chrisp et al., 2001). Therefore, as shown in Figure 8, there is no general tendency for the activation energy changes with FTCs, which varies with *w*/*c* and NaCl solution concentration. According to the results, it seems the variation of activation energy due to FTCs is not significant in the case of *w*/*c* = 0.3 and 0.5, but the decrease of activation energy in the case of *w*/*c* = 0.7 and 15% NaCl solution saturated sample cannot be simply neglected.

3.4 Elastic modulus changes with FTCs

After certain FTCs, the samples were taken out of the environment chamber and then the three-point bending test was conducted, as shown in Figure 3. The elastic modulus was calculated based on Eq. (2). The ratio of elastic modulus of sample after FTCs to before FTCs was defined as normalized elastic modulus. The results were shown in Figure 9. From the figures, the mechanical degradation can be observed clearly in *w*/*c* = 0.5 and 0.7. In particular, the 5% NaCl case reduced progressively with FTCs, and finally it has the most severe damage. This can be explained by the combined effect of ice nucleation and salt crystallization (Wu et al., 2014). The ice expansion can cause destructive damage in mortar and reduce its elastic modulus. However, the amount of ice in the case of 5% NaCl is less than DI water in theory (Wang, Gong, Zhang, & Ueda, 2016d), which cannot cause very severe damage. According to Wu et al. (2014) study, after salt frost damage of concrete, the Friedel's salt was detected. So, it was believed that this salt crystallization also contribute to the damage of mortar in addition to the ice formation.

3.5 Freezing and thawing points change with FTCs

With regard to Figure 5, the freezing and thawing points with FTCs were detected and are shown in Figures 10 and 11, respectively. The freezing point of solution in mortar depends on the pore size and solution concentration. After frost damage, the porosity and connectivity would increase, which means that the pore size can increase, consequently the freezing and thawing points may increase. However, as shown in Figure 10, no obvious freezing point change tendency can be observed. Although the variation exists, it may be due to the heterogeneous ice nucleation nature (Zeng, Li, & Fen-Chong, 2015). The freezing and thawing points decrease with the NaCl solution concentration. With different *w*/*c*, the trend is not clear, we can see that *w*/*c* = 0.5 has the lowest freezing point in the case of DI water, whereas they are in the same range for the other cases.

It seems that the thawing point of sample was steady compared with freezing point. For the DI water case, the thawing point increases with *w*/*c*, which means the macro pore size is bigger in higher *w*/*c*. But for 5% and 15% NaCl solution cases, this conclusion may not be appropriate because of the pore solution concentration and possible salt crystallization. When the NaCl penetrates into mortar, the formation of Friedel's salt could occur and fill the pores, altering the pore size of mortar (Wang et al., 2016c). With increasing NaCl solution concentration and *w*/*c*, the amount of Friedel's salt increases (Wang et al., 2016a). Therefore, for 5 and 15% NaCl solution saturated samples, the macro pore size is not bigger in higher *w*/*c*.

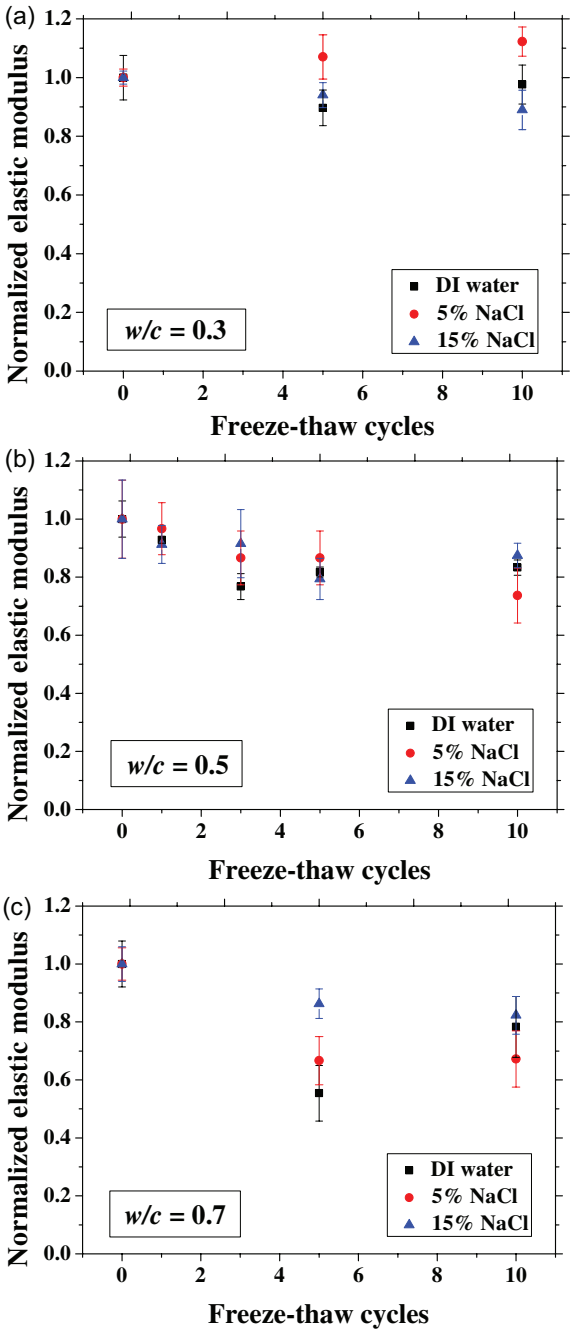

Figure 9. Normalized elastic modulus changes with FTCs. (a) *w*/*c* = 0.3, (b) *w*/*c* = 0.5, and (c) *w*/*c* = 0.7.

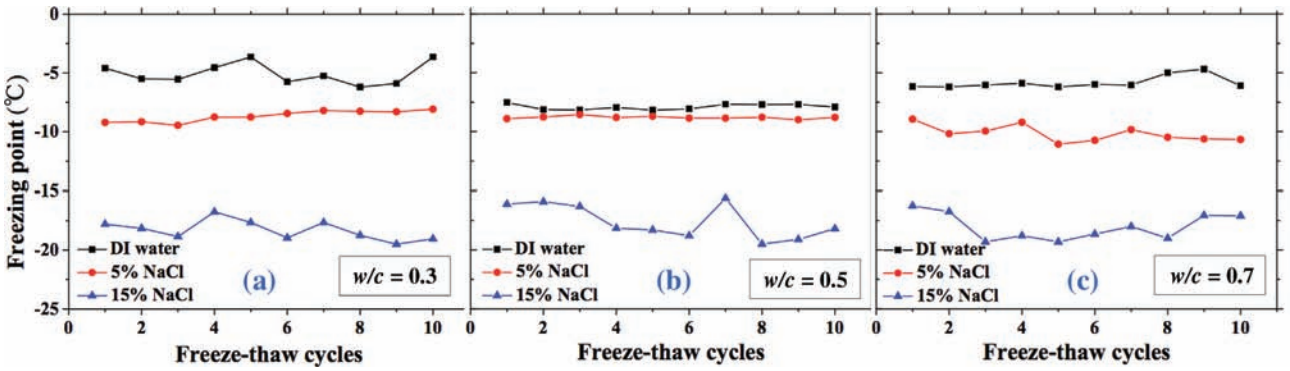

Figure 10. Freezing point changes with FTCs. (a) *w*/*c* = 0.3, (b) *w*/*c* = 0.5, and (c) *w*/*c* = 0.7.

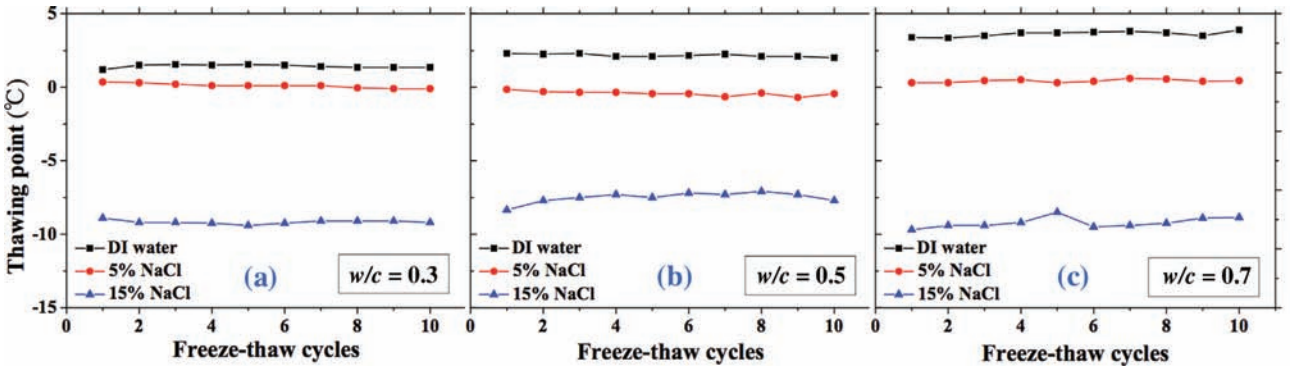

Figure 11. Thawing point changes with FTCs. (a) *w*/*c* = 0.3, (b) *w*/*c* = 0.5, and (c) *w*/*c* = 0.7.

4. CONCLUSIONS

In this paper, the electrical response of mortar in mesoscale saturated with DI water, 5 and 15% NaCl solutions under FTCs was studied. From the discussion, the following conclusions could be reached:

(1) In sealed condition, under FTCs, the specimens saturated with NaCl solutions could be severely damaged. Both of the electrical resistivity at highest and lowest temperatures changes with the damage development. But none of them alone agree with the elastic modulus degradation well, which means the evaluation parameter needs further investigation.

(2) Activation energy of mortar is not steady with frost damage development, and the variation is not significant. To develop an evaluation model, it increases with reduction of saturation degree and decreases with increasing of porosity and connectivity should be taken into consideration.

(3) Freezing and thawing points were detected from the relationship between electrical resistivity and temperature. From the previous report, the freezing point increases with FTCs. But in our mesoscale test results, such tendency was not observed.

ACKNOWLEDGMENTS

The authors would like to express their sincere thanks to the Grant-in-Aid for Scientific Research (A) of Japan Society of Promotion of Science (No. 26249064) and Research Fund of Ministry of transport construction technology, China (2014318494020). The first author would also like to show his gratitude to the scholarship granted by Chinese Scholarship Council (CSC) which supports the author's PhD study and research work.

REFERENCES

ACI Committee. (1991). *Standard practice for selecting proportions for normal, heavyweight, and mass concrete (ACI 211.1–91)*. Farmington Hills, MI, author.

Baroghel-Bouny, V., Wang, X., Thiery, M., Saillio, M., & Barberon, F. (2012). Prediction of chloride binding isotherms of cementitious materials by analytical model or numerical inverse

analysis. *Cement and Concrete Research, 42*(9), 1207–1224.

Cai, H., & Liu, X. (1998). Freeze-thaw durability of concrete: Ice formation process in pores. *Cement and Concrete Research, 28*(9), 1281–1287.

Chrisp, T., Starrs, G., McCarter, W., Rouchotas, E., & Blewett, J. (2001). Temperature-conductivity relationships for concrete: An activation energy approach. *Journal of Materials Science Letters, 20*(12), 1085–1087.

Farnam, Y., Bentz, D., Sakulich, A., Flynn, D., & Weiss, J. (2014). Measuring freeze and thaw damage in mortars containing deicing salt using a low temperature longitudinal guarded comparative calorimeter and acoustic emission (AE-LGCC). *Journal of Advances in Civil Engineering Materials (ASTM), 3*(1), 316–337.

Farnam, Y., Todak, H., Spragg, R., & Weiss, J. (2015). Electrical response of mortar with different degrees of saturation and deicing salt solutions during freezing and thawing. *Cement and Concrete Composites, 59*(0), 49–59.

Gong, F., Wang, Y., Zhang, D., & Ueda, T. (2015). Mesoscale simulation of deformation for mortar and concrete under cyclic freezing and thawing stress. *Journal of Advanced Concrete Technology, 13*(6), 291–304.

JCI Standard. (2003). *Method of test for fracture energy of concrete by use of notched beam. JCI-S-001-2003*. Tokyo, Japan, author.

Litvan, G. G. (1976). Frost action in cement in the presence of de-icers. *Cement and Concrete Research, 6*(3), 351–356.

Liu, Y., & Presuel-Moreno, F. J. (2014). Normalization of temperature effect on concrete resistivity by method using Arrhenius law. *ACI Materials Journal, 111*(4), 433–442.

Liu, Z., & Hansen, W. (2015). Freezing characteristics of air-entrained concrete in the presence of deicing salt. *Cement and Concrete Research, 74*(0), 10–18.

Sato, T., & Beaudoin, J. J. (2011). Coupled AC impedance and thermomechanical analysis of freezing phenomena in cement paste. *Materials and Structures, 44*(2), 405–414.

Sun, Z., & Scherer, G. W. (2010). Effect of air voids on salt scaling and internal freezing. *Cement and Concrete Research, 40*(2), 260–270.

Valenza, J. J., & Scherer, G. W. (2007). A review of salt scaling: II. Mechanisms. *Cement and Concrete Research, 37*(7), 1022–1034.

Wang, Z., Zeng, Q., Wang, L., Yao, Y., & Li, K. (2014). Electrical resistivity of cement pastes undergoing cyclic freeze-thaw action. *Journal of Materials in Civil Engineering, 27*(1), 04014109.

Wang, Y., Gong, F., Ueda, T., & Zhang, D. (2016a). Meso-scale mechanical degradation of mortar under freeze thaw cycles and sodium chloride attack. *Proceedings of the 11th fib international PhD symposium in civil engineering*. Tokyo, Japan, University of Tokyo.

Wang, Y., Gong, F., Zhang, D., & Ueda, T. (2016b). Estimation of ice content in mortar based on electrical measurements under freeze-thaw cycle. *Journal of Advanced Concrete Technology, 14*(2), 35–46.

Wang, Y., Gong, F., Zhang, D., & Ueda, T. (2016c). Mesoscale study of water transport in mortar influenced by sodium chloride. *Journal of Asian Concrete Federation*. (under review).

Wang, Y., Gong, F., Zhang, D., & Ueda, T. (2016d). Estimation of ice formation in cementitious materials saturated with sodium chloride solutions. *Proceedings of the 14th East Asia-Pacific conference on structural engineering and construction (EASEC-14)*. Ho Chi Minh City, Vietnam.

Weiss, J., Snyder, K., Bullard, J., & Bentz, D. (2012). Using a saturation function to interpret the electrical properties of partially saturated concrete. *Journal of Materials in Civil Engineering, 25*(8), 1097–1106.

Whittington, H., McCarter, J., & Forde, M. (1981). The conduction of electricity through concrete. *Magazine of Concrete Research, 33*(114), 48–60.

Wu, Z., Shi, C., Gao, P., Wang, D., & Cao, Z. (2014). Effects of deicing salts on the scaling resistance of concrete. *Journal of Materials in Civil Engineering, 27*(5), 04014160.

Zeng, Q., Fen-Chong, T., & Li, K. (2014). Freezing behavior of cement pastes saturated with NaCl solution. *Construction and Building Materials, 59*, 99–110.

Zeng, Q., Li, K., & Fen-Chong, T. (2015). Heterogeneous nucleation of ice from supercooled NaCl solution confined in porous cement paste. *Journal of Crystal Growth, 409*, 1–9.